



S77C-ΔC7-CueR: a $^{199\text{m}}\text{Hg}$ PAC study of the protein metal site structure

R. K. Balogh¹ · A. Jancso¹ · B. Gyurcsik¹ · J. Schell^{2,3} · J. G. Correia⁴ · P. W. Thulstrup⁵ · L. Hemmingsen⁵

Accepted: 23 February 2024
© The Author(s) 2024

Abstract

The CueR protein regulates the cytosolic concentration of Cu(I) in bacteria such as *E. coli*. With this work we aimed to remodel the linear two-coordinate metal site with Cys112 and Cys120 as ligands in CueR to a tricoordinate site similar to that observed in the Hg(II) sensor protein MerR. This was done by introducing an additional cysteine near the metal site in the modified S77C-ΔC7-CueR variant, inspired by the fact that Ser77 in CueR is replaced by a cysteine in MerR. $^{199\text{m}}\text{Hg}$ PAC spectroscopic data indicate that two NQIs are present at pH 8.0, most likely reflecting HgS₂ and HgS₃ coordination modes, and demonstrating that the design of a pure HgS₃ metal site was not achieved. Lowering the pH to 6.0 or the temperature to -196 °C had surprisingly similar effects, giving rise to highly distorted trigonal Hg(II) coordination. Tentatively, this might reflect that the histidine just next to Cys77 (His76) coordinates forming a HgS₂N metal site structure. Further redesign beyond the first coordination sphere appears to be required to efficiently stabilize the HgS₃ metal site structure at physiological pH.

Keywords Cu(I) · Hg(II) · Metal ion sensor protein · Metal site structure

✉ L. Hemmingsen
lhe@chem.ku.dk

¹ Department of Molecular and Analytical Chemistry, University of Szeged, Szeged, Hungary

² Institute for Materials Science and Center for Nanointegration Duisburg-Essen (CENIDE), University of Duisburg-Essen, Duisburg, Germany

³ European Organization for Nuclear Research (CERN), CH-1211 Geneva, Switzerland

⁴ Centro de Ciências e Tecnologias Nucleares (C2TN), Instituto Superior Técnico, DECN, Universidade de Lisboa, Lisbon, Portugal

⁵ Department of Chemistry, University of Copenhagen, Copenhagen, Denmark

1 Introduction

The dimeric CueR protein is a transcriptional regulator, which controls the concentration of Cu(I) in, for example, *E. coli* [1]. CueR binds Cu(I) in a linear structure with two coordinated thiolates [1]. We have previously explored the binding of Hg(II) to CueR and to a variant missing the last seven (C-terminal) amino acid residues, $\Delta C7$ -CueR [2, 3]. The two cysteines within the seven C-terminal residues (CCHHRAG) exhibit the capacity to coordinate to Hg(II) in addition to the two cysteines (Cys112 and Cys120) forming the native Cu(I) metal site. With the current project, we aimed to transform the metal site structure of CueR to a site with three cysteines, potentially creating a Hg(II) sensor protein. Moreover, we aimed to avoid the interference from the cysteines from the C-terminal fragment. Therefore, we used the $\Delta C7$ -CueR variant as a starting point. Next, we redesigned the $\Delta C7$ -CueR protein by mutating Ser77 to Cys. Ser77 (from the other monomer) is located spatially in close proximity to the metal site [1], and introducing a Cys at this position potentially creates a HgS_3 metal ion binding site with three thiolates, akin to the Hg(II) sensor protein MerR [4–7]. The idea of mutating Ser77 to Cys and thereby altering the specificity of CueR was also pursued by Ibáñez et al. [8], demonstrating that the S77C-CueR protein activates transcription both in the presence of Cu(I) and Hg(II), but no experimental characterization of the metal site structure in the presence of Hg(II) was presented. Here we characterize the metal site structure of S77C- $\Delta C7$ -CueR using ^{199m}Hg PAC spectroscopy. PAC spectroscopy has been applied in biochemistry for decades, and for a general overview of such applications we refer the reader to the literature [9, 10].

2 Methods

2.1 Protein expression, purification, and quality control

The S77C- $\Delta C7$ -CueR protein was expressed and purified in the same manner as $\Delta C7$ -CueR, as described in [2] and [3]. Quality control including purity, DNA binding and secondary structure characterization of the protein is also described in [3], see also the [supporting information](#).

2.2 PAC spectroscopy

The protein samples were prepared as described in [2]. The experiments were carried out at the CERN/ISOLDE laboratories, and conducted on an analogue 6-detector PAC instrument (PERM, time per channel of 0.05019 ns), except for the experiment with a sample temperature of -196 °C, for which a digital instrument (DIGIPAC, time per channel of 0.04883 ns) was applied. The conventional data analysis (t_0 determination and subtraction of background chance coincidences for coincidence spectra for each detector pair) was conducted to generate, $R(t)$, the experimental equivalent of the perturbation function [9]. The production of the radioisotope ^{199m}Hg is outlined in [11]. 300 data points (up to ca. 15 ns of $R(t)$), were used in the data analysis, except the first 10 data points (up to ca. 0.5 ns of $R(t)$) due to systematic errors (caused by small variations in t_0 for coincidence spectra for each detector pair), still below the experimental time resolution of $t_{res} = 0.51$ ns. The fitting

Table 1 Parameters fitted to the $^{199\text{m}}\text{Hg}$ PAC spectra. a: fixed in the fit. Experimental conditions are described in the captions of Fig. 1 (the first two entries of this table) and Fig. 2 (the last four entries of this table). Standard deviations are indicated in parenthesis

Sample	Temp. (°C)	Equiv. Hg(II)	pH	ν_Q (GHz)	η	$A \times 100$
$\Delta\text{C7-CueR}$ [2]	1	0.2	8.0	1.55(1)	0.16(3)	14(1)
$\text{S77C-}\Delta\text{C7-CueR}$	1	0.2	8.0	1.65(3) 1.15(1)	0(1) 0.23(6)	11(3) 5(2)
$\text{S77C-}\Delta\text{C7-CueR}$	1	0.01	8.0	1.66(3) 1.14(1)	0(1) 0.24(7)	9(3) 5(2)
$\text{S77C-}\Delta\text{C7-CueR}$	1	0.2	6.0	1.56(6) 1.13(2)	0.1(2) 0.53(4)	7(2) 6(1)
$\text{S77C-}\Delta\text{C7-CueR}$	-196	0.2	8.0	1.65 ^a 1.14(2)	0.2(1) 0.50(3)	2(1) 13(1)

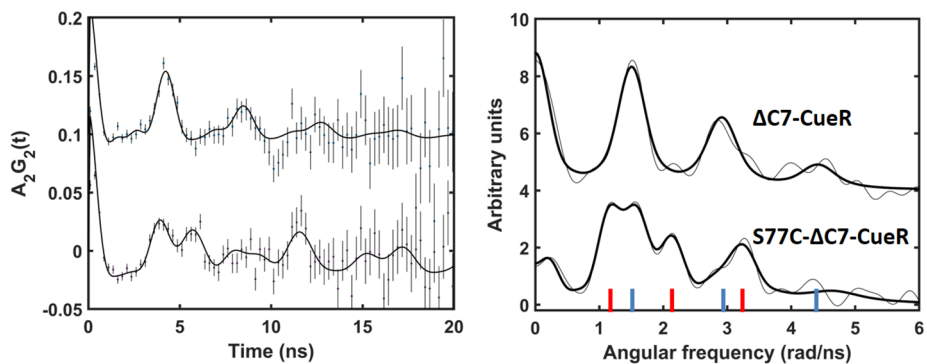


Fig. 1 $^{199\text{m}}\text{Hg}$ PAC spectra recorded for the $\Delta\text{C7-CueR}$ (upper spectrum, from [2]) and the $\text{S77C-}\Delta\text{C7-CueR}$ (lower spectrum) variant of the CueR protein. Left: $R(t)$ (to facilitate visual inspection, each point in the figure is the average of five data points, and data from $\Delta\text{C7-CueR}$ are shifted vertically by 0.1 on the $A_2G_2(t)$ scale) and fit (full line); Right: Fourier transformed data (thin line) and fit (bold faced line). The two NQIs are indicated in blue (NQI1) and red (NQI2) in the plot of the Fourier transformed data. Conditions: 20 μM protein monomer, 4 μM Hg(II), 10 μM DNA, 20 mM Tris, pH=8.0, 55% sucrose, 1 °C

function for each NQI (for a PAC isotope with spin, $I=5/2$, in the intermediate state of the γ - γ -cascade) is:

$$R(t) = A_2^{eff} e^{-\lambda t} \left(a_0 + \sum_{i=1}^3 a_i \cos(\omega_i t) e^{-\frac{(\omega_i t_{res})^2}{16 \ln(2)}} e^{-\omega_i \delta t} \right)$$

Where A_2^{eff} (indicated as A for each species in Table 1) is the effective amplitude (or anisotropy), λ accounts for stochastic dynamics, such as rotational diffusion of the labelled molecule in solution, a_i and ω_i depend on the ν_Q and η , and therefore on the local structure at the PAC probe site, and δ reflects so-called static variations of the NQI. Due to limited signal-to-noise ratio for the current data, reliable fitting of the baseline was difficult, and this in turn affects the fitted amplitudes and λ . This does not significantly affect the conclusions presented in this work.

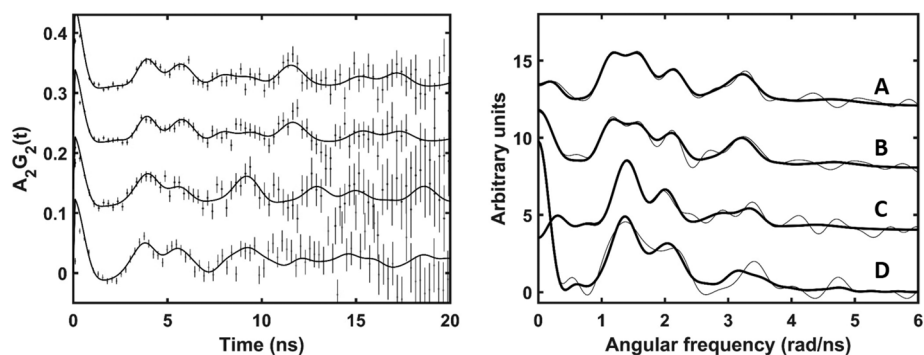


Fig. 2 $^{199\text{m}}\text{Hg}$ PAC spectra recorded for the S77C- Δ C7-CueR variant of the CueR protein. Left: $R(t)$ (to facilitate visual inspection, each point in the figure is the average of five data points, and data are shifted vertically on the $A_2G_2(t)$ scale for experiments A, B, and C) and fit (full line); Right: Fourier transformed data (thin line) and fit (bold faced line). Conditions: 20 μM protein monomer, 10 μM DNA, 55% sucrose, and A: 4 μM Hg(II), 20 mM Tris, pH=8.0, 1 $^\circ\text{C}$; B: 0.2 μM Hg(II), 20 mM Tris, pH=8.0, 1 $^\circ\text{C}$; C: 4 μM Hg(II), 20 mM MES, pH=6.0, 1 $^\circ\text{C}$; D: 4 μM Hg(II), 20 mM Tris, pH=8.0, -196 $^\circ\text{C}$ (deviations from our standard experimental conditions is indicated by underline)

3 Results and discussion

Figure 1 and the first two entries in Table 1 display $^{199\text{m}}\text{Hg}$ PAC data for Δ C7-CueR and S77C- Δ C7-CueR under the same experimental conditions. As demonstrated previously, Hg(II) binds to Δ C7-CueR in a linear HgS_2 coordination geometry [2], and this $^{199\text{m}}\text{Hg}$ PAC spectrum is included as a reference in Fig. 1. The metal site structure in S77C- Δ C7-CueR is more complex, see Fig. 1, and displays the presence of two NQIs. Fitting the spectrum is not trivial, but one component, very similar to that reported for Δ C7-CueR (NQ1), may be included, indicating linear HgS_2 coordination. The second NQI (NQI2) gives parameters similar to those reported previously for trigonal planar HgS_3 coordination [11], see Fig. 3A. The fits presented in Fig. 1 and Table 1 follow this interpretation, and the frequencies of the two NQIs are indicated in Fig. 1 as blue (NQI1) and red (NQI2) lines in the plot of the Fourier transformed data. It is possible to fit NQI1 in a different manner, assuming η close to 1 (rather than the low η for the fit presented in Table 1). However, including the high η NQI1 in the fit instead of the low η NQI1, leads to a low total amplitude (around 0.08), and for $^{199\text{m}}\text{Hg}$ and the given instrument and typical sample volumes, the total effective amplitude should be around 0.14, so the high η NQI1 was discarded. In principle, the amplitudes of NQI1 and NQI2 directly reflect the population of HgS_2 and HgS_3 coordination modes. However, due to relatively poor signal-to-noise ratio at long times (>15 ns after the detection of the first γ) in each of the 30 individual coincidence spectra, the baseline is poorly determined, and this may affect the reported amplitudes.

In summary, the most straightforward interpretation of the $^{199\text{m}}\text{Hg}$ PAC data recorded for S77C- Δ C7-CueR is that two coordination geometries, a distorted linear HgS_2 and a distorted trigonal planar HgS_3 , co-exist under our experimental conditions. A similar equilibrium between HgS_2 and HgS_3 was observed in the *de novo* designed trimeric coiled coil TRIL9C at essentially the same pH (7.9) by $^{199\text{m}}\text{Hg}$ PAC and $^{199\text{m}}\text{Hg}$ NMR spectroscopy [11], corroborating that such an equilibrium may exist at this pH. The MerR protein, which is a natural Hg(II) sensor, exhibits HgS_3 coordination as characterized by $^{199\text{m}}\text{Hg}$ PAC [6]

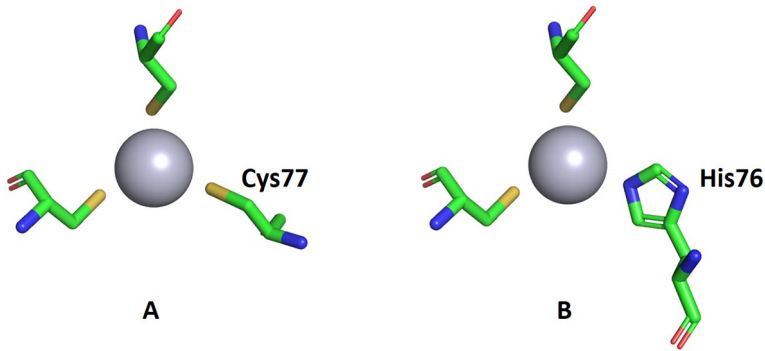


Fig. 3 Models of metal site structures introduced by the Ser77Cys mutation (i.e. new structures observed for the S77C- Δ C7-CueR variant of the CueR protein). A: Introduction of Cys77 near the metal site gives rise to a trigonal planar HgS₃ metal site (at pH 8.0, this NQI is indicated by red lines in Fig. 1), which co-exists with the HgS₂ metal site (this NQI is indicated by blue lines in Fig. 1) present in the “mother” protein (Δ C7-CueR). B: A HgS₂N metal site, with His76 as the third ligand might tentatively give rise to the PAC signal at lower pH (6.0) or lower temperature (77 K), where the asymmetry parameter, η , increases significantly

and ¹⁹⁹Hg NMR spectroscopy [7]. Thus, although the desired HgS₃ coordination mode does appear to exist for Hg(II) bound to S77C- Δ C7-CueR, remodeling of the metal site to a pure HgS₃ structure was not obtained. This observation implies, that remodeling of the metal site surroundings beyond the first coordination sphere is required, to form a pure HgS₃ metal site coordination geometry at this pH.

Figure 2 and the last three entries in Table 1 display additional experimental ^{199m}Hg PAC data and fits, where the experimental conditions were changed as outlined in the following. Figure 2A shows the same spectrum as the bottom spectrum in Fig. 1, i.e. S77C- Δ C7-CueR. Spectrum ‘B’ in Fig. 2 represents data for an experiment with only 0.2 μ M Hg(II) (0.01 equiv. per protein monomer). The possibility to go to very low concentrations of the PAC probe is one of the advantages of the technique, and here essentially no change is observed with respect to spectrum ‘A’ in Fig. 2, and correspondingly the fitted PAC parameters presented in Table 1 (entries 2 and 3) are highly similar. This demonstrates that a 20 fold reduction of Hg(II) concentration, and thus in the Hg(II)-to-protein ratio, does not alter the speciation. I.e. the same two NQIs are observed, and their relative population is essentially the same. This observation indicates that the equilibrium between the two species (giving rise to NQI1 and NQI2) cannot originate from a reaction involving binding of a second Hg(II) ion to the protein, but may reflect an equilibrium involving a conformational change, such as association/dissociation of a single ligand, at the metal site. This agrees well with the interpretation presented above, that NQI1 and NQI2 originate from HgS₂ and HgS₃, respectively.

Experiments conducted on *de novo* designed trimeric coiled coils have demonstrated that decreasing pH may stabilize HgS₂ coordination over HgS₃ coordination [11], because protonation of the third thiolate occurs under slightly acidic/close to neutral conditions in the presence of Hg(II) ions. We aimed to explore if a similar transition to HgS₂ coordination occurred for Hg(II)-S77C- Δ C7-CueR when lowering pH to 6. The ^{199m}Hg PAC spectrum ‘C’ in Fig. 2 was recorded for S77C- Δ C7-CueR at lower pH (pH 6.0), and a change with respect to spectrum ‘A’ is observed. However, one might have expected to observe a pure

HgS₂ species at pH 6.0, and that is clearly not the case (as compared to Fig. 1, top spectrum). Moreover, the asymmetry parameter, η , of the low frequency NQI changes significantly from 0.24 at pH 8.0 to 0.53 at pH 6.0, indicating a loss of axial symmetry. It has been demonstrated that the protein remains stable in the presence of DNA [12], so this change of PAC spectroscopic signature is unlikely to reflect protein unfolding. A Tentative interpretation might be, that the histidine next to the S77C mutation (His76) coordinates. In an ideal HgS₃ trigonal planar structure there is axial symmetry along the axis perpendicular to the HgS₃ plane, in agreement with the relatively low value of $\eta=0.24$ at pH 8.0 for NQI2. However, coordination by His76 would form a HgS₂N metal site, breaking the axial symmetry, in agreement with the higher value of $\eta=0.53$ at pH 6.0, see Fig. 3B.

Finally, changing the temperature may shift the equilibrium between HgS₂ and HgS₃ coordination, potentially leading to pure HgS₃ coordination at lower temperature. Thus, an experiment was conducted with the sample temperature at -196 °C (liquid nitrogen), see Fig. 2D. The fit to this data set is not fully satisfactory, and might reflect the presence of a third NQI, but the signal-to-noise ratio does not allow for reliable identification of a NQI3. Interestingly, the spectrum is similar to that recorded at pH 6.0, implying that lowering the temperature might lead to formation of a HgS₂N metal site via coordination by His76, see Fig. 3B. However, this is highly speculative, partly because it was necessary to fix the frequency (ν_Q) of NQI1 in the fit, and this leads to lower amplitude of this fitted NQI1.

Supplementary Information The online version contains supplementary material available at <https://doi.org/10.1007/s10751-024-01879-0>.

Acknowledgements We acknowledge the financial support received from the Federal Ministry of Education and Research (BMBF) through grants 05K16PGA and 05K22PGA. We also acknowledge the support of all the technical teams at ISOLDE for their excellent work in delivering high-quality beams for PAC measurements. We acknowledge the funding from the Danish National center for CERN Experiments (NICE). We acknowledge the support of the European Union's Horizon Europe Framework research and innovation programme under grant agreement no. 101057511 (EURO-LABS).

Author contributions R.K.B, A.J, B.G., P.W.T and L.H. wrote the main manuscript text and prepared the supplementary material. R.K.B, A.J, B.G., J.S., J.G.C. and P.W.T. performed the experiments. All authors reviewed the manuscript.

Funding Open access funding provided by Copenhagen University. European Union's Horizon 2020 Framework research and innovation program under grant agreement no. 654002 (ENSAR2) and Fundação para a Ciência e a Tecnologia (FCT), Portugal under grant CERN/FIS-TEC/0003/2021 and UIDB/04349/2020.

Data availability After publication, the data will be stored at Zenodo.

Declarations

Ethical approval Not applicable.

Competing interests The authors declare no competing interests.

Open Access This article is licensed under a Creative Commons Attribution 4.0 International License, which permits use, sharing, adaptation, distribution and reproduction in any medium or format, as long as you give appropriate credit to the original author(s) and the source, provide a link to the Creative Commons licence, and indicate if changes were made. The images or other third party material in this article are included in the article's Creative Commons licence, unless indicated otherwise in a credit line to the material. If material is not included in the article's Creative Commons licence and your intended use is not permitted

by statutory regulation or exceeds the permitted use, you will need to obtain permission directly from the copyright holder. To view a copy of this licence, visit <http://creativecommons.org/licenses/by/4.0/>.

References

1. Changela, A., Chen, K., Xue, Y., Holschen, J., Outten, C.E., O'Halloran, T.V., Mondragón, A.: *Science*. **301**, 1383–1387 (2003)
2. Balogh, R.K., Gyurcsik, B., Hunyadi-Gulyás, É., Schell, J., Thulstrup, P.W., Hemmingsen, L., Jancsó, A.: *Chem. Eur. J.* **25**, 15030–15035 (2019)
3. Balogh, R.K.: PhD thesis, University of Szeged, Hungary, (2020)
4. Helmann, J.D., Ballard, B.T., Walsh, C.T.: *Science*. **247**, 946–948 (1990)
5. Chang, C.-C., Lin, L.-Y., Zou, X.-W., Huang, C.-C.: *N -L Chan Nucleic Acids Res.* **43**, 7612–7623 (2015)
6. Lippert, C., Tröger, W., Butz, T.: *Proceedings of XXX Zakopane School of Physics, Zakopane, Poland*, Eds. K. Tomala and E.A. Görlich, p. 339–343. (1995)
7. Utschig, L.M., Bryson, J.W., O'Halloran, T.V.: *Science*. **268**, 380–385 (1995)
8. Ibáñez, M.M., Checa, S.K.: *F C Soncini J. Bacteriol.* **197**, 1606–1613 (2015)
9. Hemmingsen, L., Sas, K.N.: *E Danielsen Chem. Rev.* **104**, 4027–4061 (2004)
10. Chakraborty, S., Pallada, S., Pedersen, J.T., Jancso, A., Correia, J.G., Hemmingsen, L.: *Acc. Chem. Res.* **50**, 2225–2232 (2017)
11. Iranzo, O., Thulstrup, P.W., Ryu, S., Hemmingsen, L., Pecoraro, V.L.: *Chem. Eur. J.* **13**, 9178–9190 (2007)
12. Balogh, R.K., Németh, E., Jones, N.C., Hoffmann, S.V., Jancsó, A., Gyurcsik, B.: *Eur. Biophys. J.* **50**, 491–500 (2021)

Publisher's Note Springer Nature remains neutral with regard to jurisdictional claims in published maps and institutional affiliations.